Thermal stability of artinite, dypingite and brugnatellite- implications for the geosequestration of green house gases

Ray L. Frost, • **Silmarilly Bahfenne, Jessica Graham and Wayde N. Martens**

Inorganic Materials Research Program, School of Physical and Chemical Sciences, Queensland University of Technology, GPO Box 2434, Brisbane Queensland 4001, Australia.

Abstract

The approach to remove green house gases by pumping liquefied carbon dioxide several kilometres below the ground implies that many carbonate containing minerals will be formed. Among these minerals the formation of dypingite, artinite and if the ferric iron is present brugnatellite are possible; thus necessitating a study of the thermal stability of such minerals. The thermal stability of two carbonate bearing minerals dypingite and artinite together with brugnatellite with a hydrotalcite related formulae have been characterised by a combination of thermogravimetry and evolved gas mass spectrometry. Artinite is thermally stable up to 352°C. Two mass loss steps are observed at 219 and 355 °C. Dypingite decomposes at a similar temperature but over a large number of steps. Brugnatellite shows greater stability with decomposition not occurring until after 577°C. The thermal decomposition of brugnatellite occurs over a number of mass decomposition steps. It is concluded that pumping liquefied green house gases into magnesium bearing mineral deposits is feasible providing a temperature of 350-355 °C is not exceeded to prevent escape of CO_2 towards the surface. In contrast, the water loss occurring at lower temperatures could have a positive effect on the geosequestration of CO_2 as it probably causes a decrease in the molar volume of secondary carbonate minerals and consequently an increase in aquifer porosity.

Key words: artinite, dypingite, brugnatellite, carbonate, thermal stability, thermogravimetry, thermal analysis, geological sequestration of CO_2

• Author to whom correspondence should be addressed (r.frost@qut.edu.au)

Introduction

The ability to be able to easily and readily detect minerals is of importance [1, 2]. This is especially so where carbonate minerals are concerned. What is probably not appreciated is that many carbonate containing minerals especially the secondary minerals are soluble and can be decomposed upon heating. The proposal to remove green house gases by pumping liquid-like CO_2 in deep aquifers (> 800 m approx.), chiefly hosted in sedimentary basins, is expected to cause formation of many carbonate containing minerals [3-6]. Two magnesium carbonate minerals which may form under such conditions of high CO_2 partial pressure are dypingite $Mg_5(CO_3)_4(OH)_2.5H_2O$ [7-11] and artinite $Mg_2(CO_3)(OH)_2.3H_2O$ [12-21]. Other magnesium containing minerals are the ferric ion bearing minerals coalingite $Mg_{10}Fe^{3+}_2(CO_3)(OH)_{24}\cdot 2(H_2O)$,[22-29] and brugnatellite $Mg_6Fe^{3+}(CO_3)(OH)_{13}\cdot 4(H_2O)$ [27, 30-34] and hydrotalcite $Mg_6Al_2(CO_3)(OH)_{16}\cdot 4(H_2O)$. The formulae of these first two minerals appear to be related to that of hydrotalcites. Pastor-Rodriguez and Taylor reported the crystal structure of coalingite and presented a model coalingite with a d(003) spacing of 1.25 nm [29]. Brugnatellite is related to the manasseite-pyroaurite mineral group [$Mg_6R^{3+}_2(CO_3)(OH)_{16}\cdot 4(H_2O)$, where R^{3+} = Al, Cr or Fe].

The study of the magnesium carbonates is of extreme importance in the development of technology for the removal of green house gases. Magnesium minerals such as brucite, periclase and several Mg-silicates (e.g., the serpentine group minerals, forsterite, etc.) have the potential for the sequestration of carbon dioxide. Hydrotalcites may also be used but must be first thermally activated [35]. Studies of the thermodynamic [6] and phase diagrams [13] of related magnesium minerals have been published [36] .The reaction path involving carbonation of brucite ($Mg(OH)_2$) is particularly complex, as Mg has a strong tendency to form a series of metastable hydrous carbonates. These metastable hydrous carbonates include hydromagnesite ($Mg_5(CO_3)_4(OH)_2.4H_2O$, artinite ($Mg_2CO_3(OH)_2.3H_2O$), nesquehonite ($MgCO_3.3H_2O$), and lansfordite ($MgCO_3.5H_2O$). The free energy of formation for

these hydroxy and hydrous carbonates differs and their generation depends on the partial pressure of CO_2 [6].

Thermal analysis using thermogravimetric techniques enables the mass loss steps, the temperature of the mass loss steps and the mechanism for the mass loss to be determined [37-43]. Thermoanalytical methods provide a measure of the thermal stability of the hydrotalcite and related minerals. Structural information on different minerals has successfully been obtained recently by sophisticated thermal analysis techniques [37-42]. In this work we report the thermal analysis of the magnesium carbonate minerals artinite, dypingite and coalingite

Experimental

Minerals

The following minerals were used in this research (a) Dypingite - Yoshikawaite, Shinshiro Shi, Aichi Prefecture, Japan (b) Sample 4 Dypingite - Clear Creek District, Southern San Benito County, California (c) Sample 3 Artinite - Clear Creek District, Southern San Benito County, California (d) Sample 7 Artinite - Higasi-Kuroda-Guchi, Inasa-Cho, Inasa-Gun, Aichi Prefecture, Japan.
The origin of the brugnatellite minerals is as follows: (e) Brugnatellite - Monte, Ramazzo, Genoa, Liguria, Italy; (f) Brugnatellite - Higasi-Kuroda-Guchi, Inasa-Cho, Inasa-Gun, Aichi Prefecture, Japan. The minerals are associated with iron-containing brucite.

Thermal analysis

Thermal decomposition of the magnesium carbonates was carried out in a TA® Instruments incorporated high-resolution thermogravimetric analyzer (series Q500) in a flowing nitrogen atmosphere (60 cm^3 min^{-1}). Approximately 35 mg of sample underwent thermal analysis, with a heating rate of 5°C min^{-1}, and high resolution, to 1000°C. With the heating program of the instrument the furnace temperature was regulated precisely to provide a uniform rate of decomposition in the main decomposition stage. The TGA instrument was coupled to a Balzers (Pfeiffer) mass

spectrometer for gas analysis. Only water vapour, carbon dioxide and oxygen were analyzed.

Results and Discussion

In order to make a study of the potential of these carbonate minerals for geosequestration it is important to use the natural minerals. Thus there may arise differences between the experimental mass losses and the theoretical mass losses, because of (a) impurities in the minerals (b) partial dehydration. It is worthwhile noting that there have been detailed studies of artinite including the thermodynamic properties [44, 45]. The comment may be also made that there have been no thermodynamic or detailed studies on dypingite and brugnatellite.

The thermogravimetric and differential thermogravimetric analysis of artinite $Mg_2CO_3(OH)_2.3H_2O$ is shown in Figure 1. The ion current curves for the evolved gas analysis are displayed in Figure 2. Two mass loss steps at 219 and 352°C with mass losses of 26 and 24 % are observed. The following reactions are proposed for the thermal decomposition of artinite:

At 219 °C, $Mg_2CO_3(OH)_2.3H_2O \rightarrow Mg_2CO_3(OH)_2 + 3H_2O$ (1)

At 352°C, $Mg_2CO_3(OH)_2 \rightarrow 2\ MgO + CO_2 + H_2O$ (2)

The thermogravimetric and differential thermogravimetric analysis for artinite clearly shows that water is lost at 219°C. The ion current curves suggest water is lost at 169, 218 and 218 °C. Some water vapour is measured at 341 °C. The ion current curves prove that CO_2 is evolved at 355, 393 and 429 °C. The theoretical mass loss for the first reaction, the dehydration step is 27 %. The observed mass loss of 26 % is comparable. It is proposed in reaction 2 that decarbonation and dehydroxylation take place simultaneously. The theoretical mass loss for dehydroxylation is 8.67% and for decarbonation is 22 %. Thus the theoretical mass loss is ~31%. The observed mass loss at 352°C is 24 %. Two small mass losses at 393 and 428°C of 2.7 and 2.6 % are observed. The total observed mass loss over the 300 to 500°C is 29 % which is comparable with the calculated expected mass loss.

References to previous studies on the thermal decomposition of artinite are very few. Beck [46] reported the DTA patterns of artinite. In the DTA, Beck reported the decomposition to start at 230°C with the loss of 'water of crystallisation' with a maximum at 280°C. Dehydroxylation was found to occur at 385°C and decarbonation at 540°C. The DTA pattern reported by Beck (page 1001) shows strong asymmetry and may indicate a rapid heating rate which has skewed the DTA patterns. This results in the displacement of the temperatures of the thermal decomposition to higher temperatures than might be found if the heating rate was significantly less. The observation by Beck that the dehydroxylation occurs at 280°C fits reasonably well with the dehydration temperature of 219°C. Beck also indicated that dehydroxylation and decarbonation overlapped. This observation fits well with the DTG peak at 352°C.

The thermal decomposition of dypingite $Mg_5(CO_3)_4(OH)_2.5H_2O$ is reported in Figure 3. The ion current curves for the evolved gases from the dypingite sample are reported in Figure 4. Four mass loss steps at 70, 108, 182 and 213 °C are observed with a total mass loss of 8 %. This value is less than the calculated value of 18 %. This difference is attributed to the presence of other minerals in the dypingite mineral sample. The observation of four mass loss steps suggests the water is lost in steps. The ion current curves for dypingite show that water is lost at 53, 105, 210 and 346 °C, this confirming that water is lost in stages. It is possible that water is lost as high as 353 °C. Two mass decomposition steps at 353 and 383 °C are observed and are attributed to partial dehydration and dehydroxylation. The mass loss at 567 °C is assigned to the decarbonation and partial dehydroxylation of the dypingite. . The calculated mass loss is 10 % which is close to the observed value of 8 %. To the best of the authors knowledge there have been few reported thermal analyses of dypingite as compared with some other magnesium carbonate minerals [8, 10].

The thermal analysis of the mineral brugnatellite $Mg_6Fe^{3+}(CO_3)(OH)_{13}.4H_2O$ is shown in Figure 5. The ion current curves are reported in Figure 6. The ion current curves for H_2O shows that water is evolved at 67, 118, 245, 297, 349 and 579 °C. The ion current curves for CO_2 show that this gas is evolved at predominantly 336, 354 and 422 °C. This latter peak maximum is broad and covers a wide temperature range. This shows that the decomposition of the brugnatellite takes place over a wide

temperature range. Thermally induced mass loss steps are observed at 68, 119, 247, 300, 348 and 577°C. The first two mass loss steps are ascribed to dehydration with a mass loss of 4 % which can not be compared with the calculated value of 13 %. The mass loss at 247 °C is a dehydroxylation step. The mass loss at 348 °C attributed to a combination of decarbonation and dehydroxylation is 8 %. The mass loss at 577 °C is 8.6 % and is assigned based upon the ion current curves to decarbonation. The mass loss of CO_2 at 577 °C is 9 % as compared with the calculated value of 8 % based upon the formula $Mg_6Fe^{3+}(CO_3)(OH)_{13}.4H_2O$. It is concluded that dehydration, dehydroxylation, and decarbonation are occurring over several temperature ranges and there is no clear peak that can be assigned to any of these processes.

Possible chemical reactions

In order to understand the potential chemical reactions of green house gases through reaction with magnesium minerals, it is important to set up model reactions and to understand these reactions. In this work, we have used the reaction of CO_2 with brucite and periclase as model reactions. In reality reaction of CO_2 with many compounds of Mg including silicates will need to be studied. It is important to have fundamental knowledge of the reactions of $Mg(OH)_2$ and MgO with CO_2 [36, 47]. It is important to understand that the conditions of the reaction will affect the products in the following reactions [36]. Botha and Strydom showed that the reaction conditions including slurry pH, slurry temperature, drying temperature, drying time influence the product formation [36].

The following reactions may be envisaged: $MgO + CO_2 \rightarrow MgCO_3$ and

$2MgO + CO_2 + 4H_2O \rightarrow Mg_2CO_3(OH)_2.3H_2O$ (artinite)

$5MgO + 4CO_2 + 6H_2O \rightarrow Mg_5(CO_3)_4(OH)_2.5H_2O$ (dypingite)

$6MgO + Fe^{3+} + CO_2 + 9H_2O + 3OH^- \rightarrow Mg_6Fe^{3+}(CO_3)(OH)_{13}.4H_2O$ (brugnatellite)

It is important to understand the stability of such minerals both in terms of temperature and partial pressure of the CO_2 [13]. The hydration-carbonation or hydration-and-carbonation reaction path in the CO_2—MgO—H_2O system at ambient temperature and atmospheric CO_2 is of practical significance from the standpoint of carbon balance and the removal of green house gases from the atmosphere. A better

200 understanding of the global masses of Mg and CO_2 and the thermal stability of the
201 hydrated carbonates of magnesium provide a practical understanding for carbon
202 dioxide removal. From a practical point of view, the exact knowledge of the reaction
203 path in MgO—CO_2—H_2O system is of great significance to the performance of
204 $Mg(OH)_2$ and related minerals for green house gas removal. The reaction path
205 involving carbonation of brucite ($Mg(OH)_2$) is particularly complex, as Mg has a
206 strong tendency to form a series of metastable hydrous carbonates. These metastable
207 hydrous carbonates include hydromagnesite ($Mg_5(CO_3)_4(OH)_2.4H_2O$, or
208 $Mg_4(CO_3)_3(OH)_2.3H_2O$), artinite ($Mg_2CO_3(OH)_2.3H_2O$), dypingite
209 $Mg_5(CO_3)_4(OH)_2.5H_2O$, nesquehonite ($MgCO_3.3H_2O$), and lansfordite
210 ($MgCO_3.5H_2O$) and if Fe^{3+} is present and available then minerals such as brugnatellite
211 and coalingite may be formed. The free energy of formation for these hydroxy and
212 hydrous carbonates differs and their formation will depend on the partial pressure of
213 CO_2.
214
215 **Conclusions**
216
217 The potential for using magnesium ore deposits for the geosequestration of
218 green house gases is real. Such a system will depend at least in part on the formation
219 of a range of magnesium carbonate minerals including artinite, dypingite and
220 brugnatellite. This work has shown that dehydration of these minerals occurs at 219 °C
221 for artinite, 213 °C for dypingite and 247 °C for brugnatellite, whereas decarbonation
222 takes place at 350-355°C for the three magnesium hydroxyl-carbonate minerals. Water
223 loss and CO_2 loss from these solid phases upon heating have different impact on the
224 geosequestration of CO_2 through injection of liquid-like CO_2 in deep aquifers, chiefly
225 hosted in sedimentary basins. The first process (water loss) could have a positive
226 effect as it probably causes a decrease in the molar volume of secondary hydroxyl-
227 carbonate minerals and consequently an increase in aquifer porosity, whereas the
228 second process (CO_2 loss) has a negative effect (owing to the possible escape of the
229 CO_2 towards the surface) and must absolutely be avoided.
230
231
232 **Acknowledgments**
233

The financial and infra-structure support of the Queensland University of Technology, Inorganic Materials Research Program is gratefully acknowledged. The Australian Research Council (ARC) is thanked for funding the instrumentation.

References

[1] G.R. Hunt, R.P. Ashley, Economic Geology and the Bulletin of the Society of Economic Geologists 74 (1979) 1613-1629.

[2] G.R. Hunt, R.C. Evarts, Geophysics 46 (1981) 316-321.

[3] J.W. Anthony, R.A. Bideaux, K.W. Bladh, M.C. Nichols, Handbook of Mineralogy, Mineral Data Publishing, Tiscon, Arizona, USA, 2003.

[4] L.B. Railsback, Carbonates and Evaporites 14 (1999) 1-20.

[5] S.W.M. Blake, C. Cuff, Preparation and use of cationic halides, sequestration of carbon dioxide. (Perma-Carb Pty Ltd, Australia). Application: WO WO, 2007, p. 66pp.

[6] L. Marini, Geological sequestration of carbon dioxide: Thermodynamics, kinetics, and reaction path modeling. , Elsevier, 2007.

[7] P.P. Smolin, T.A. Ziborova, Doklady Akademii Nauk SSSR 226 (1976) 923-926 [Mineral].

[8] G.O. Nechiporenko, G.V. Sokolova, T.A. Ziborova, G.P. Bondarenko, Mineralogicheskii Zhurnal 10 (1988) 78-85.

[9] J.H. Canterford, G. Tsambourakis, B. Lambert, Mineralogical Magazine 48 (1984) 437-442.

[10] P.J. Davies, B. Bubela, Chemical Geology 12 (1973) 289-300.

[11] G. Raade, American Mineralogist 55 (1970) 1457-1465.

[12] H.G.M. Edwards, S.E.J. Villar, J. Jehlicka, T. Munshi, Spectrochimica Acta, Part A: Molecular and Biomolecular Spectroscopy 61A (2005) 2273-2280.

[13] E. Konigsberger, L.-C. Konigsberger, H. Gamsjager, Geochimica et Cosmochimica Acta 63 (1999) 3015-3119.

[14] M. Akao, S. Iwai, Acta Crystallographica, Section B: Structural Crystallography and Crystal Chemistry B33 (1977) 3951-3953.

[15] J.R. Guenter, H.R. Oswald, Journal of Solid State Chemistry 21 (1977) 211-215.

[16] K.N. Goswami, Indian Journal of Pure and Applied Physics 12 (1974) 667-669.

[17] H. Jagodzinski, Mineral. Petrog. Mitt. 10 (1965) 297-330.

[18] M. deWolff, Acta Cryst. 5 (1952) 286-287.

[19] M. Fenoglio, Periodico di Mineralogia 13 (1942) 1-10.

[20] L. Brugnatelli, Centr. Min. 35 (1903) 144-148.

[21] L. Brugnatelli, Rend. Ist. Lombardo 35 (1902) 869-874.

[22] S. Caillere, Compt. rend. 219 (1944) 256-258.

[23] H. Delnavaz, R. Allmann, Zeitschrift fuer Kristallographie 183 (1988) 175-178.

[24] C. Frondel, American Mineralogist 26 (1941) 295-315.

[25] O.K. Ivanov, Materialy po Mineral. Mestorozhd. Urala, Sverdlovsk (1984) 75-78.

[26] J.L. Jambor, American Mineralogist 54 (1969) 437-447.

[27] H. Kolmer, W. Postl, Mitteilungsblatt - Abteilung fuer Mineralogie am Landesmuseum Joanneum 45 (1977) 137-141.

[28] F.A. Mumpton, H.W. Jaffe, C.S. Thompson, American Mineralogist 50 (1965) 1893-1913.

[29] J. Pastor-Rodriguez, H.F.W. Taylor, Mineralogical Magazine and Journal of the Mineralogical Society (1876-1968) 38 (1971) 286-294.

[30] E. Artini, Atti della Accademia Nazionale dei Lincei, Classe di Scienze Fisiche, Matematiche e Naturali, Rendiconti 18 (1910) 3-6.
[31] S. Caillere, Bull. soc. franc, mineral. 66 (1943) 494-502.
[32] M. Fenoglio, Rev. geol. 19 (1938) 128.
[33] I.E. Grey, R. Ragozzini, Journal of Solid State Chemistry 94 (1991) 244-253.
[34] H.F.W. Taylor, Mineralogical Magazine and Journal of the Mineralogical Society (1876-1968) 37 (1969) 338-342.
[35] R.L. Frost, A.W. Musumeci, M.O. Adebajo, W. Martens, Journal of Thermal Analysis and Calorimetry 89 (2007) 95-99.
[36] A. Botha, C.A. Strydom, Hydrometallurgy 62 (2001) 175-183.
[37] R.L. Frost, K.L. Erickson, J. Therm. Anal. Calorim. 76 (2004) 217-225.
[38] E. Horvath, J. Kristof, R.L. Frost, N. Heider, V. Vagvoelgyi, J. Therm. Anal. Calorim. 78 (2004) 687-695.
[39] R.L. Frost, M.L. Weier, K.L. Erickson, J. Therm. Anal. Calorim. 76 (2004) 1025-1033.
[40] R.L. Frost, K.L. Erickson, J. Therm. Anal. Calorim. 78 (2004) 367-373.
[41] E. Horvath, J. Kristof, R.L. Frost, A. Redey, V. Vagvolgyi, T. Cseh, J. Therm. Anal. Calorim. 71 (2003) 707-714.
[42] J. Kristof, R.L. Frost, J.T. Kloprogge, E. Horvath, E. Mako, J. Therm. Anal. Calorim. 69 (2002) 77-83.
[43] R.L. Frost, W. Martens, Z. Ding, J.T. Kloprogge, J. Therm. Anal. Calorim. 71 (2003) 429-438.
[44] H.C. Helgeson, J.M. Delany, H.W. Nesbitt, D.K. Bird, Summary and critique of the thermodynamic properties of rock-forming minerals, 1978.
[45] J.M. Delany, H.C. Helgeson, American Journal of Science 278 (1978) 638-686.
[46] C.W. Beck, American Mineralogist 35 (1950) 985-1013.
[47] R.A. Robie, B.S. Hemingway, Thermodynamic properties of minerals and related substances at 298.15K and 1 Bar (105 Pascals) pressure and at higher temperatures. . 1995.

List of Figures

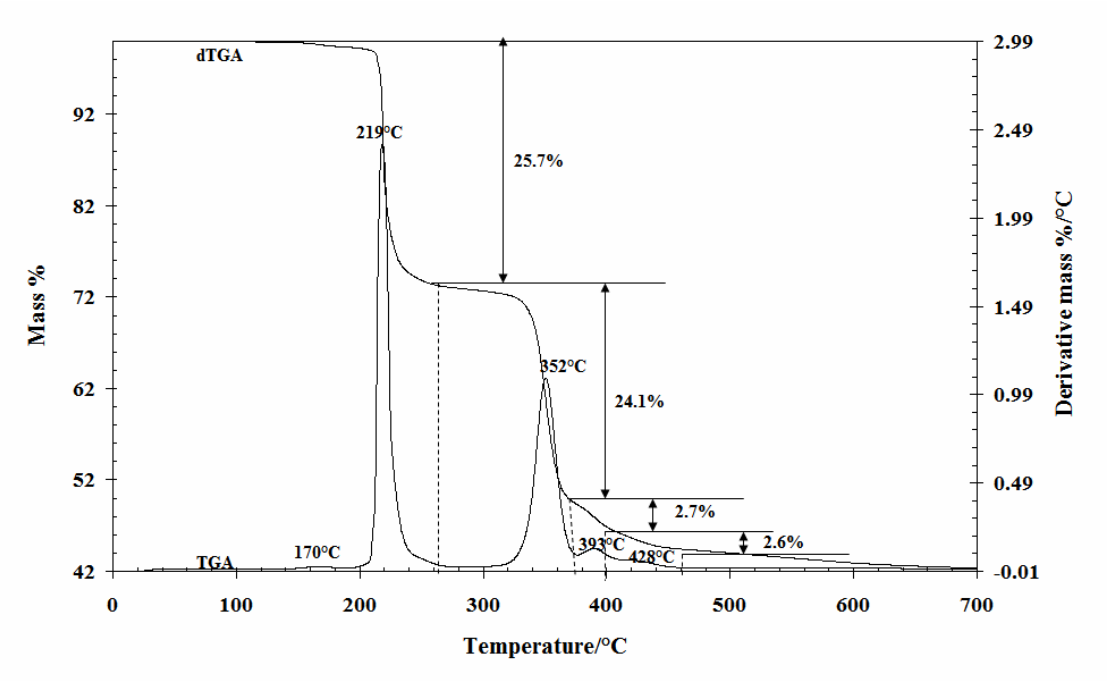

335

336

337 **Figure 1**

338

339

340

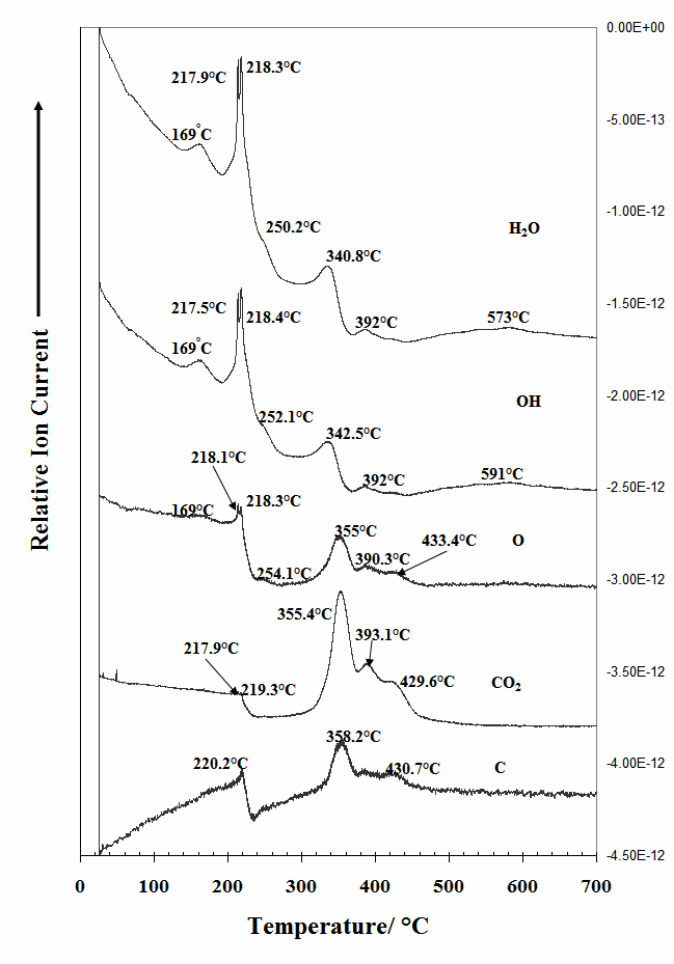

341

342

343 **Figure 2**

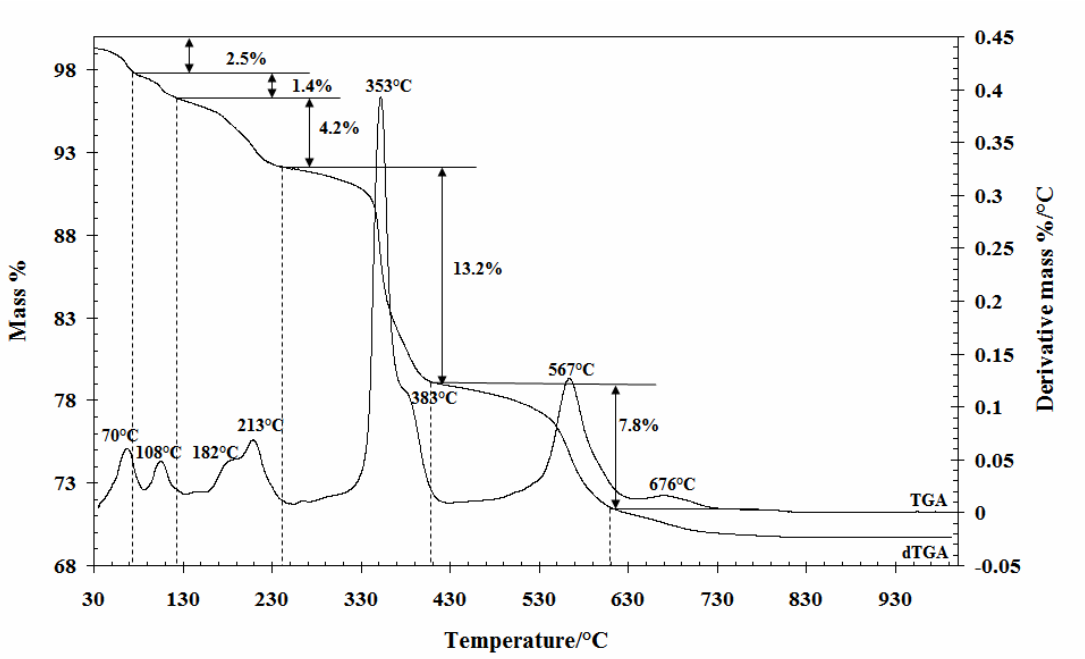

344

345

346 **Figure 3**

347

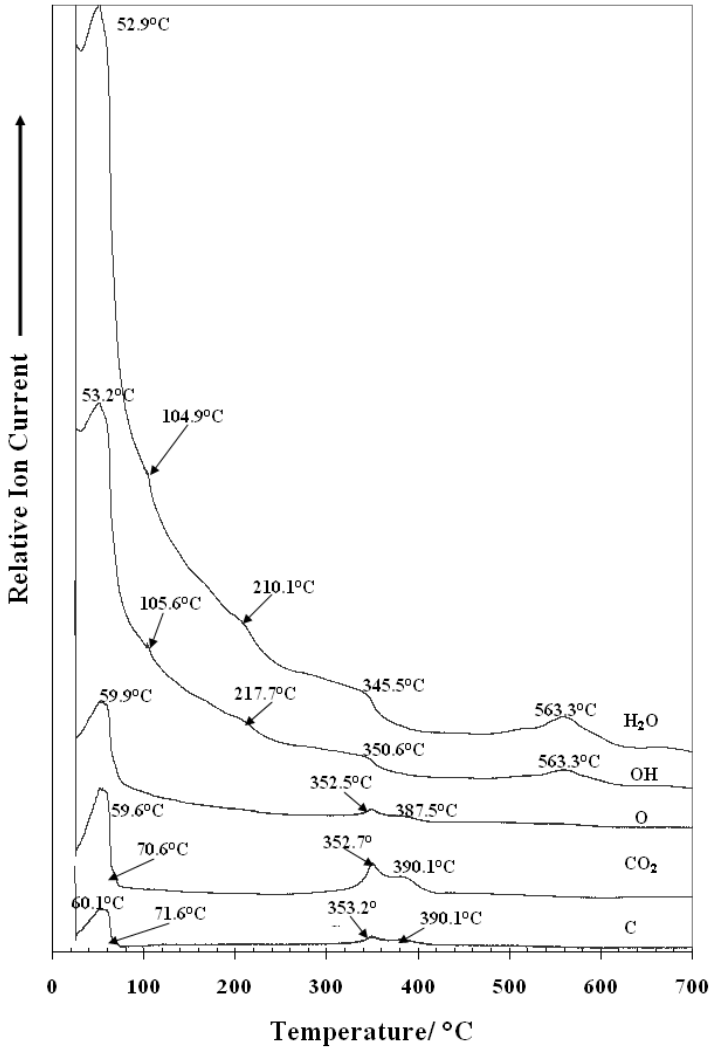
52.9°C
53.2°C
104.9°C
210.1°C
105.6°C
345.5°C
59.9°C
217.7°C
563.3°C
H2O
350.6°C
563.3°C
OH
352.5°C
59.6°C
387.5°C
O
70.6°C
352.7°
390.1°C
CO2
60.1°C
71.6°C
353.2°
390.1°C
C
Relative Ion Current
0
100
200
300
400
500
600
700
Temperature/ °C

Figure 4

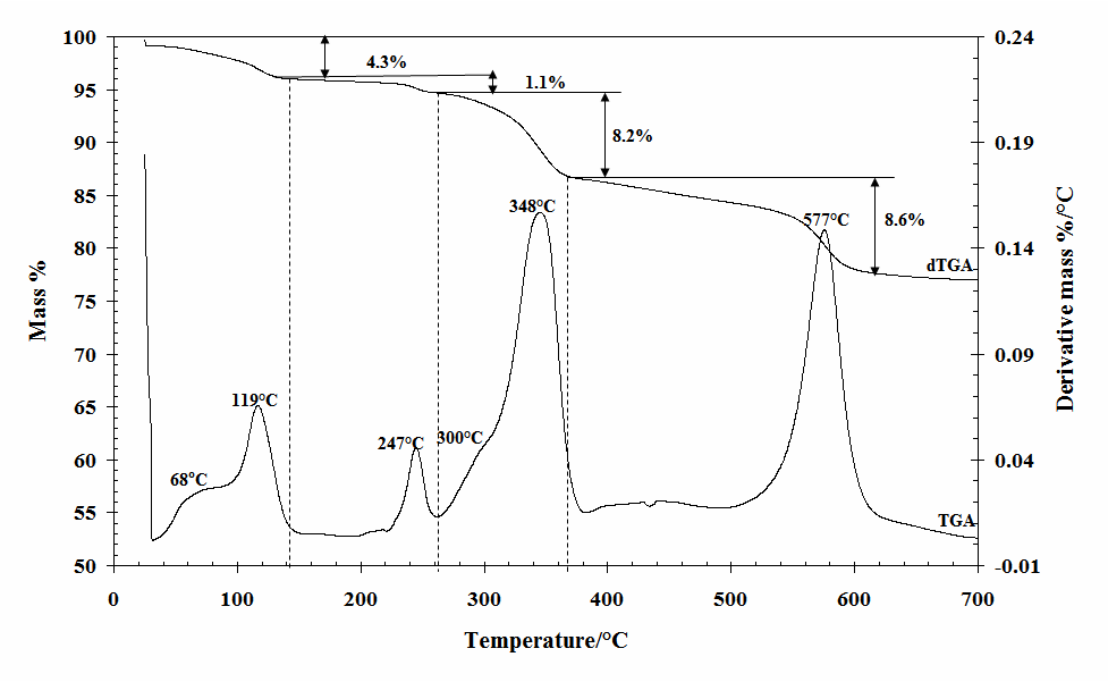

356

357

358 **Figure 5**

359

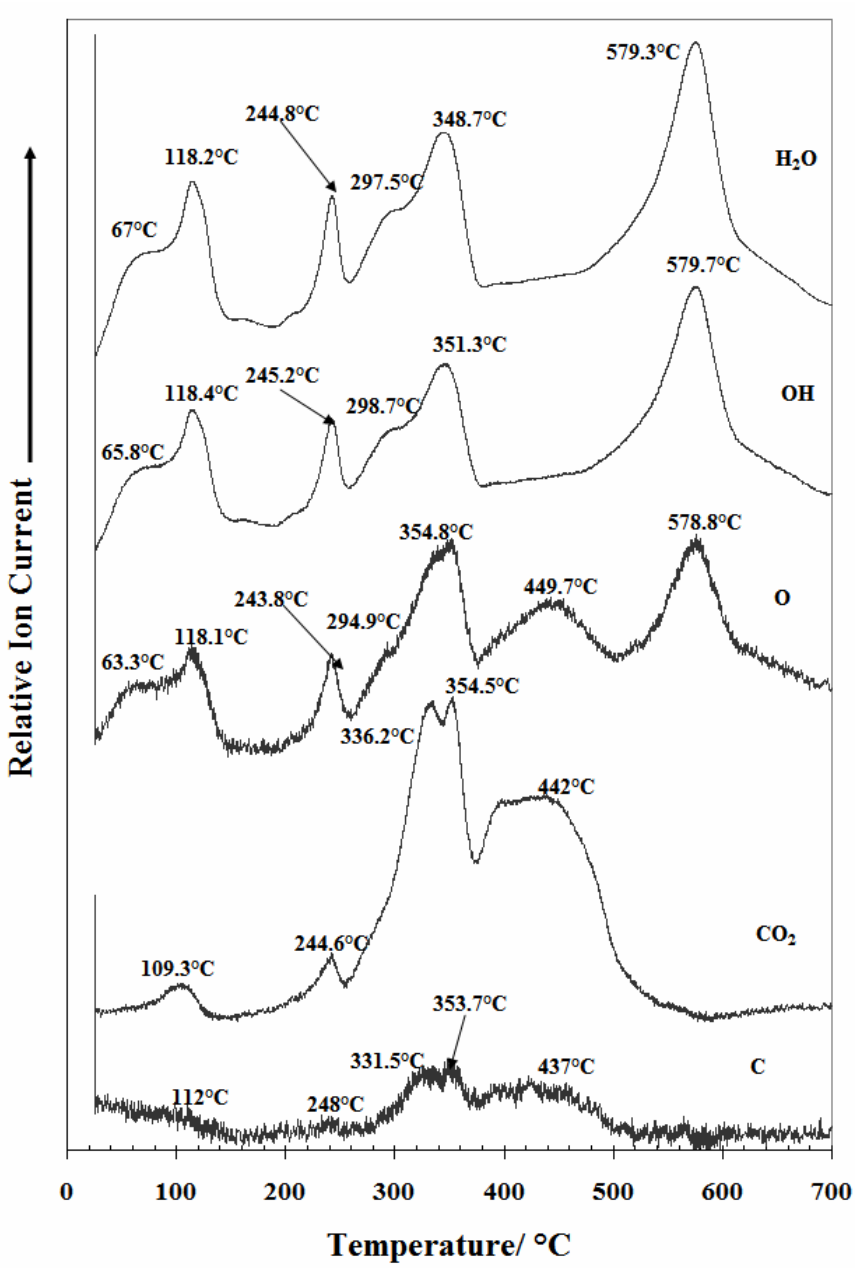

360

361

362 **Figure 6**